

## Evaluation of New Scaffolds of Myeloperoxidase Inhibitors by Rational Design Combined with High-Throughput Virtual Screening

Iyas Aldib,<sup>†</sup> Jalal Soubhye,<sup>†</sup> Karim Zouaoui Boudjeltia,<sup>§</sup> Michel Vanhaeverbeek,<sup>§</sup> Alexandre Rousseau,<sup>§</sup> Paul G. Furtmüller,<sup>||</sup> Christian Obinger,<sup>||</sup> Francois Dufrasne,<sup>†</sup> Jean Nève,<sup>†</sup> Pierre Van Antwerpen,<sup>\*,†,#,‡</sup> and Martine Prévost<sup>‡,#</sup>

<sup>†</sup>Laboratoire de Chimie Pharmaceutique Organique, Faculté de Pharmacie, Université Libre de Bruxelles, Brussels, Belgium

<sup>‡</sup>Analytical Platform of the Faculty of Pharmacy, Université Libre de Bruxelles, Brussels, Belgium

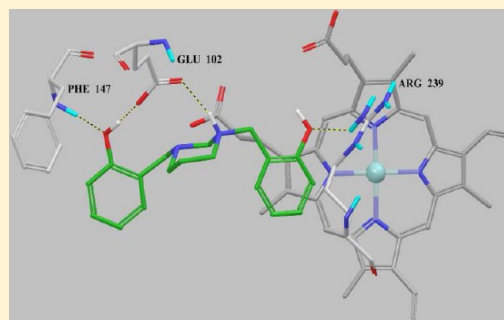
<sup>§</sup>Laboratory of Experimental Medicine, CHU Charleroi, A. Vesale Hospital, Université Libre de Bruxelles, Montigny-le-Tilleul, Belgium

<sup>||</sup>Department of Chemistry, Division of Biochemistry at the Vienna Institute of BioTechnology, BOKU—University of Natural Resources and Life Sciences, Muthgasse 18, A-1190 Vienna

<sup>‡</sup>Laboratoire de Structure et Fonction des Membranes Biologiques, Université Libre de Bruxelles, Brussels, Belgium

### **S** Supporting Information

**ABSTRACT:** Myeloperoxidase (MPO) is a major player of the innate immune defense system of human neutrophils and catalyzes the production of strong oxidizing and halogenating antimicrobial products. Because of its role in pathogenesis of many (inflammatory) diseases, there is great interest in the development of efficient and specific inhibitors. Here, using the X-ray structure of MPO, high-throughput molecular docking of 1350000 compounds was performed. From this virtual screening process, 81 were tested for inhibition of the chlorination activity of MPO, finally ending up with eight inhibiting candidates of different chemical structures. These were tested for inhibiting MPO-mediated low-density lipoprotein oxidation and for interacting with the relevant redox intermediates of MPO. The best inhibitors were bis-2,2',2''-[(dihydro-1,3(2*H*,4*H*)-pyrimidinediyl)bis-(methylene)]phenol and 8-[(2-aminoethyl)amino]-3,7-dihydro-3-methyl-7-(3-phenoxypropyl)-1*H*-purine-2,6-dione. Both did not irreversibly inactivate the enzyme but efficiently trapped it in its compound II state. We discuss the mechanism of inactivation as well as pros and cons of the performed selection process.



### **■** INTRODUCTION

Myeloperoxidase (MPO, EC 1.11.2.2) is a major player of the antimicrobial system of mammalian neutrophils.<sup>1,2</sup> The cationic oxidoreductase belongs to the peroxidase-cyclooxygenase superfamily.<sup>3</sup> It comprises two covalently linked monomers (2 × 73 kDa) consisting of a light chain and a heavy chain that both contribute to covalent linkage with an autocatalytically modified heme group.<sup>3</sup> Myeloperoxidase is a robust enzyme that is stabilized by several disulfide bridges, one calcium ion binding site as well as five *N*-glycosylation sites per subunit.<sup>4–9</sup>

Myeloperoxidase is found in azurophil (primary) granules of neutrophils in high amounts (2–5% of total cellular protein).<sup>10,11</sup> Monocytes also contain MPO-positive granules although they are fewer in number and lost during differentiation into tissue macrophages.<sup>11,12</sup> MPO catalyzes the formation of potent oxidants such as hypochlorous acid, hypobromous acid, and hypothiocyanous acid by hydrogen peroxide (H<sub>2</sub>O<sub>2</sub>)-mediated oxidation of the corresponding (pseudo)halides.<sup>13</sup> The reaction products mediate inflammatory responses, thereby contributing to the defense system against pathogens.<sup>14,15</sup>

During oxidative stress, MPO is poured out and constitutes the so-called “circulating MPO” that might damage host tissue. It is reported that MPO plays a role in atherosclerosis, ischemia, and neurodegenerative diseases<sup>16–21</sup> as well as may influence the progression of several chronic inflammatory syndromes.<sup>14,22–25</sup> For example, MPO is not expressed in normal but in Alzheimer disease affected brain.<sup>17,20,25</sup> It was also related with some defined role in Parkinson disease and post-mortem brain regions affected by multiple sclerosis.<sup>16,26</sup> Furthermore, MPO is suggested to be involved in cardiovascular diseases and mechanistic links between MPO and atherogenesis have been intensively investigated. The peroxidase produces proatherogenic lipoproteins and induces consumption of nitric oxide (NO), thereby contributing to the development of endothelial dysfunction. Moreover, MPO initiates and propagates atheroma plaque formation and rupture, thrombosis, and ventricular remodeling.<sup>27,28</sup>

Received: May 24, 2012

Published: July 13, 2012

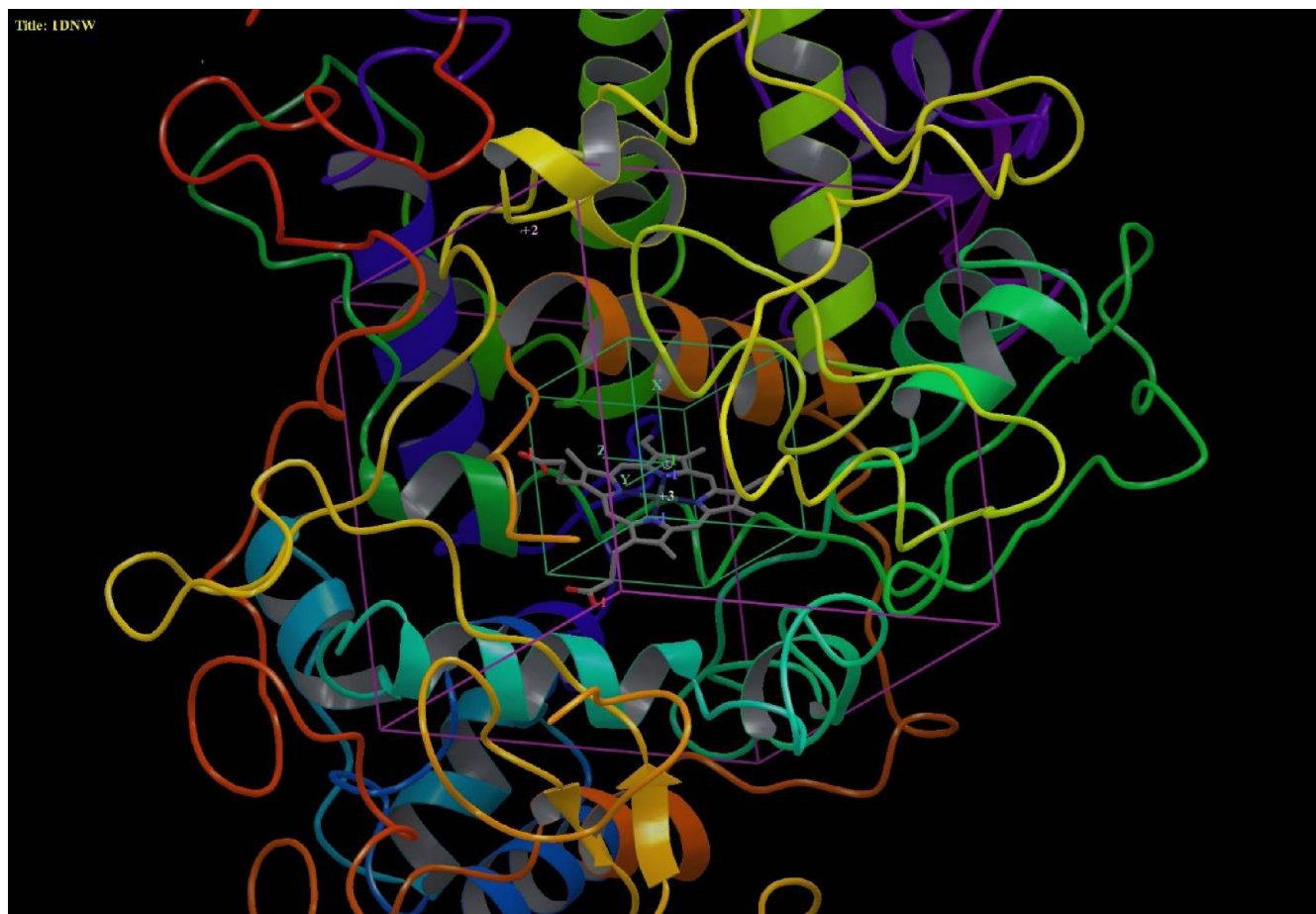


**Figure 1.** Ribbon representation of the crystal structure of the human MPO (PDB 1DNW). The heme is depicted as sticks. The inner (in green) and outer (in purple) boxes define the volume that the ligand center explores and the one in which all atoms must be located during the docking sampling.

In vitro studies have also shown that lipoproteins, modified by the MPO/H<sub>2</sub>O<sub>2</sub>/Cl<sup>-</sup> system, display a number of pathophysiological effects that contribute to the initiation and maintenance of the inflammatory process during atherosclerotic lesion development.<sup>29</sup> Low-density lipoproteins (LDLs) oxidized by this system (i.e., Mox-LDL) trigger inflammatory responses in monocytes and endothelial cells.<sup>29–36</sup> MPO was associated with progression of carotid atherosclerosis in patients with HDL cholesterol levels below 49 mg/dL.<sup>33</sup> It was also reported to have a crucial role in converting high-density lipoprotein (HDL) by selectively modifying apolipoprotein A-1 and by generating dysfunctional HDL.<sup>27,30,33–36</sup>

This close relation between MPO activity and its potential role in various diseases stimulated considerable interest in the development of therapeutic strategies to inhibit MPO catalysis. Studies have shown that a number of nonsteroidal anti-inflammatory drugs (NSAIDs) such as indomethacin, mefenamic acid, dapsone, naproxen, phenylbutazone, and sodium salicylate are valuable as MPO inhibitors in treating inflammatory syndromes.<sup>37,38</sup> Additional studies were carried out on other NSAIDs including oxim derivatives (IC<sub>50</sub> = 8–12 μM), nimesulide (IC<sub>50</sub> = 2.1 μM), and flufenamic acid (IC<sub>50</sub> = 1.8 μM), respectively,<sup>39–41</sup> but also natural compounds were reported as MPO inhibitors including quercetin (IC<sub>50</sub> = 1.27 μM).<sup>42</sup>

Many other studies refer to MPO inhibitors including hydroxamic acids such as salicylhydroxamic acid (SHA) (IC<sub>50</sub> =

3–5 μM, K<sub>D</sub> = 2 μM)<sup>43</sup> as well as benzoic acid hydrazides including 4-aminobenzoic acid hydrazide and hydroxybenzoic acid hydrazide having IC<sub>50</sub> values of 0.3 and 2 μM, respectively.<sup>44,45</sup> It was also reported that indole derivatives react with MPO and block the halogenation reaction,<sup>46,47</sup> which finally led to the finding that tryptamine derivatives such as 5-fluorotryptamine (IC<sub>50</sub> = 0.79 μM) are efficient inhibitors.<sup>48</sup> Recently, a new class of tryptamine derivatives targeting the chlorination activity of MPO was introduced.<sup>49</sup>

In parallel it has been demonstrated that 2-thioxanthine derivatives are suicide substrates of MPO, e.g., 2-isobutyl thioxanthine (IC<sub>50</sub> = 0.87 μM).<sup>50–54</sup> Other compounds that affected MPO activity were H1-antihistaminic drugs<sup>55</sup> and naphthalene derivatives, e.g., 6-methoxy-1-ethyl-3,4-dihydro-naphthalene (IC<sub>50</sub> = 3 μM).<sup>56</sup> In any case, these studies have shown that there is additional need for alternative scaffolds to conceive more efficient inhibitors with activity in the nanomolar range.<sup>57</sup>

Here, we have used a rational drug design approach based on structure-based screening of large databases of molecules. In detail, a high-throughput virtual screening (HTVS) has been performed on the public pharmaceutical database ASINEX.<sup>58</sup> Lead compounds were selected based on their scored affinities and on the predicted interactions formed with the catalytic pocket of MPO. Evaluation of data was performed by measuring the IC<sub>50</sub> values of the selected molecules for (i) inhibition of the chlorination activity and (ii) MPO-mediated

LDL oxidation. Upon using transient-state kinetic investigations of the interaction between the potential inhibitors and the various redox states of MPO, insights into the mechanism of inactivation were obtained.

## RESULTS

**High-Throughput Virtual Screening (HTVS).** Structure-based virtual screening (HTVS) was performed on the X-ray structure of human peroxidase complexed to cyanide and thiocyanate (PDB 1DNW)<sup>7</sup> using the ASINEX database<sup>58</sup> and the Glide 5.6 software from Schrodinger (Figure 1).

Three successive protocols with different levels of accuracy in the docking and scoring processes were used starting with HTVS, followed by Standard Precision (SP) and finally with eXtra Precision (XP). In detail, 1350000 compounds were docked by Glide using the HTVS mode. Ligands featuring a docking score  $< -5.5$  kcal/mol were kept. The following step was carried out by docking the selected 65006 ligands using the SP protocol, and 1000 ligands with a docking score  $< -7.8$  kcal/mol were sorted out. The final docking protocol with XP was then performed on these filtered molecules. Among the 100 best-scored compounds, 34% feature either a stacking or a shifted stacking with the heme of the protein and a salt bridge or a hydrogen bond interaction with Glu102. 45% show only one of these interactions and 21% show none of these interactions. Moreover, the 100 selected compounds consisted of 54 positively charged compounds (67%), nine negatively charged compounds (11%), and 18 neutral compounds (22%) (Figure 2).

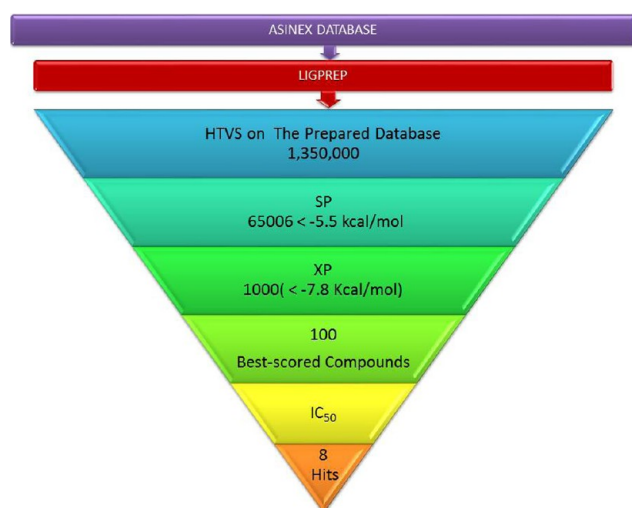


**Figure 2.** Schematic representation of the virtual screening docking protocols (HTVS, SP, and XP) starting from the ligand preparation (LIGPREP) of the compounds in the Asinex database to the selection of the best hits.

To assess the quality of the performed docking process, a set of 60 molecules of varying chemical structure and known MPO inhibiting activity was chosen from literature.<sup>37,39–49,51,56</sup> The same docking procedure was applied on these 60 ligands, which feature  $IC_{50}$  values ranging from 8 nM (3-(S-aminopentyl)-5-fluoro-1H-indole) to 30.5  $\mu$ M, (phenylbutazone).<sup>37,49</sup> After HTVS, six ligands featuring a docking score  $< -5.5$  kcal/mol were selected. These compounds ranked according to their score were 5-fluorotryptamine, 5-chlorotryptamine, SHA, 3-(S-aminopentyl)-5-fluoro-1H-indole, 3-(4-methoxybenzyl)-2-thio-

xanthine, and 3-(2-methoxy-ethyl)-2-thioxanthine. Four compounds were selected upon SP protocol. These compounds with decreasing docking score were 5-fluorotryptamine, 5-chlorotryptamine, SHA, and 3-(S-aminopentyl)-5-fluoro-1H-indole. Finally, the XP protocol produced the following order: SHA, 5-chlorotryptamine, 5-fluorotryptamine, and 3-(S-aminopentyl)-5-fluoro-1H-indole. Noticeably three out of these four compounds are analogues of indole. Concerning SHA, a crystal structure of this acid bound to MPO was determined<sup>59</sup> and made available to us by one of the authors (Davey C., private communication). By comparing the lowest-energy docked pose with the crystal structure, a root-mean-square deviation of the atomic positions of 0.5 Å was obtained, sustaining the capacity of the Glide software to retrieve the experimental position of the ligand in the MPO binding site. Noticeably, a series of known inhibitors with fairly good potency were however not selected. This outcome may be due to the well-known prevailing weakness of the scoring functions in docking programs.

Pharmacomodulation of compounds based on the 3-alkylaminoindole structure gave one of the best MPO inhibitors found so far ( $IC_{50} = 8$  nM).<sup>49</sup> Because the interactions of these derivatives with MPO are well understood, we chose 5-fluorotryptamine<sup>48,49</sup> for analysis and comparison of the interactions of the selected compounds from the screened ASINEX database (Table 1). As previously reported, docked 5-fluorotryptamine shows a stacking of the indole ring onto the pyrrole ring D of the heme. An ionic interaction between the amine and Glu102 is observed as well as one hydrogen bond with Thr100 (Figure 3).<sup>49</sup> 5-Chlorotryptamine as well as 3-(S-aminopentyl)-5-fluoro-1H-indole exhibited similar interactions.<sup>49</sup> This contrasts with the interactions formed by docked SHA where hydrogen bonds are made with Gln91 and Arg239 although its aromatic ring also stacks onto pyrrole ring D, in agreement with the crystal structure of the complex.<sup>43</sup>

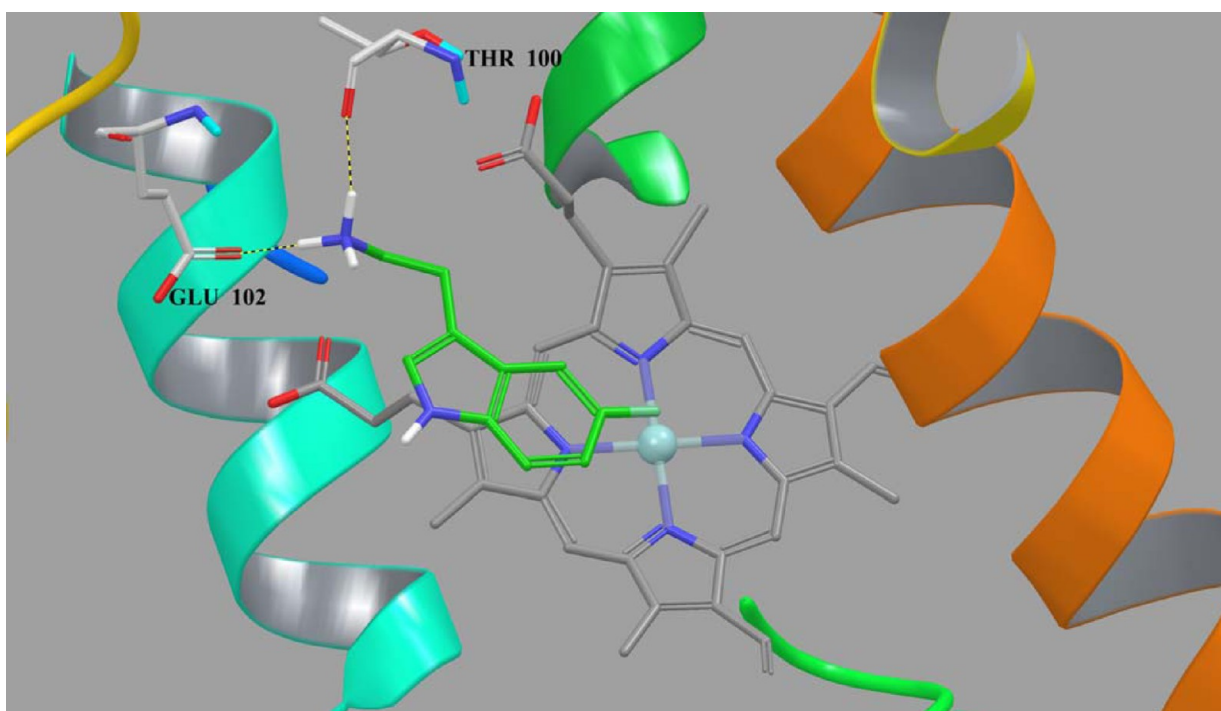
**Selection and Characterization of the Best MPO Inhibitors.** Among the 100 best compounds selected through HTVS, the activities of 81 molecules available for purchase from ASINEX were tested with a MPO inhibition assay that probed the inhibition of chlorination mediated by MPO.<sup>60</sup> Thirty-two compounds (39%) were active, but only eight compounds featuring different chemical structures and with  $IC_{50}$  values ranging between  $0.46 \pm 0.07$  and  $12 \pm 3$   $\mu$ M were selected (Table 2). Among these molecules compounds F9 ( $IC_{50} = 0.46 \pm 0.07$   $\mu$ M) and A1 ( $IC_{50} = 0.5 \pm 0.1$   $\mu$ M) are the best inhibitors. Compound C6 is slightly less active than F9 and A1 ( $IC_{50} = 0.97 \pm 0.09$   $\mu$ M). Compounds F6, C12, and F10 have about the same activity ( $IC_{50}$  3–4  $\mu$ M). Compounds A5 and D11 are active at higher concentrations (D11,  $IC_{50} = 6.2 \pm 0.5$   $\mu$ M; A5,  $IC_{50} = 12 \pm 3$   $\mu$ M). We noticed that half of the compounds are positively charged (A1, C12, F9, and F10), including the most potent inhibitors, two are neutral compounds (D11, A5) and two are negatively charged (F6, C6).

Figure 4A depicts the best score pose of compound F9, featuring a stacking of its purinedione onto the pyrrole ring D, a salt bridge with Glu102, and two hydrogen bonds with the propionate group of pyrrole ring A and Thr100 (Figure 4A). Compound A1 shows a shifted stacking of its phenyl ring with pyrrole ring D, a salt bridge with Glu102, and three hydrogen bonds with Arg239, Glu102, and Phe147 (Figure 4B). Compound F6 features one salt bridge with Glu102 and three hydrogen bonds with Glu102, Arg239, and Gln91. Its

**Table 1.** Test Results of the Three Docking Procedure Steps Performed on Known MPO Inhibitors Following the Criteria Used for the Virtual Screening (See Results)<sup>a</sup>

compound	IC <sub>50</sub> MPO inhibition assay ( $\mu$ M)	HTVS	SP	XP	refs
5-fluorotryptamine	0.79	passed	passed	passed	48
5-chlorotryptamine	0.73	passed	passed	passed	48
SHA	32	passed	passed	passed	43
3-(5-aminopentyl)-5-fluoro-1 <i>H</i> -indole	0.008	passed	passed	passed	49
3-(4-methoxybenzyl)-2-thioxanthine	0.49	passed			52, 53
3-(2-methoxy-ethyl)-2-thioxanthine	0.44	passed			52, 53
naphthalene derivatives	3–6	failed			56
oxicam group	8–12	failed			39
other NSAIDs group	0.045–30.5	failed			37, 39–41
antimalarial drugs group	0.23–1.1	failed			37
natural compounds	1.27–3	failed			42, 49
4-aminobenzoic acid hydrazide	0.3	failed			44

<sup>a</sup>The IC<sub>50</sub> values range between 0.008 and 35  $\mu$ M



**Figure 3.** Close view of the best scored 5-fluorotryptamine docked position in the catalytic site of human MPO. Its major interactions such as one salt bridge and one hydrogen bond made with residues Glu102 and Thr100, respectively, are depicted as yellow–black dotted lines.

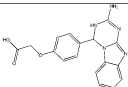
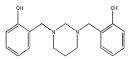
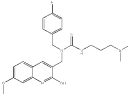
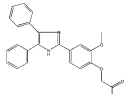
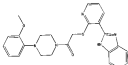
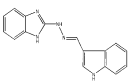
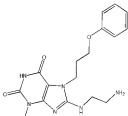
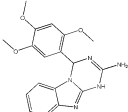
carboxylate group is oriented toward the iron atom of the heme (Figure 4C). Compound **C12** forms two hydrogen bonds with Glu102 and Arg239. The presence of a bulky substituent on this compound may hinder the formation of additional interactions with the catalytic pocket (Figure 4D). Compound **C6** makes two hydrogen bonds with residues Arg239 and Gln91. Its carboxylate group is also found to be oriented toward the iron atom in the heme (Figure 4E). Compound **D11** forms one salt bridge with Glu116 and one hydrogen bond with Glu102 (Figure 4F). Compound **A5** shows a stacking of its indole moiety with pyrrole ring D, three hydrogen bonds with the propionate group of the pyrrole ring D, Glu102, and Arg239, respectively (Figure 4G). Finally, compound **F10** shows a stacking of its benzimidazole ring with pyrrole D, one salt bridge with Glu102, and two hydrogen bonds with the propionate group of pyrrole ring A and with

Thr100 (Figure 4H) (see also Supporting Information Figure S1).

The most common interactions found among all eight docked ligands are the ionic bond with Glu102 and a stacking (shifted or not) with pyrrole ring D of the prosthetic group. Hydrogen bonds with Glu102 and with Thr100, Gln91, Arg239, or the propionate groups of the heme are also found in several docked geometries of the complexes. Interestingly, interactions with Glu102 and pyrrole ring D of the heme were also seen with fluorotryptamine derivatives that are efficient MPO inhibitors<sup>49</sup> (see Supporting Information Figure S2).

**Inhibition of LDL Oxidation.** For measuring MPO-dependent LDL oxidation, an ELISA was developed based on a mouse monoclonal antibody (Mab AG9) that specifically recognizes MPO-oxidized APO B-100 on LDL.<sup>61</sup> The eight selected compounds were tested, and MPO inhibition was probed at three different inhibitor concentrations in DMSO

**Table 2.** Lead Compounds Listed along with Their Affinity of the Best Score Docked Position (Gscore, kcal/mol), Their IC<sub>50</sub> (μM) Obtained with the MPO Inhibition Assay and the Interactions Formed within the MPO Binding Site

Formula	Gscore (kcal.mol <sup>-1</sup> )	IC <sub>50</sub> MPO inhibition assay (mean±SD μM))	Receptor-ligand interactions		
			Hydrogen bonds	Salt bridge	Stacking (S) or shift stacking (SS)
	-12.5	3.7 ± 0.8	Glu102, Arg239, Gln91	Glu102	-
	-11.6	0.5± 0.1	Glu102, Arg239, Phe147	Glu102	SS
	-10.4	3.8 ± 0.9	Glu102, Arg239	-	-
	-9.6	0.97 ± 0.09	Arg239, Gln91	-	-
	-9.6	6.2 ± 0.5	Glu102	Glu116	-
	-9.2	12 ± 3.	Glu102, Arg239, propionate ring D	-	S
	-8.9	0.46 ± 0.07	Thr100, propionate ring A.	Glu102	S
	-8.6	3.5 ± 0.3	Thr100, propionate ring A	Glu102	S

(1.25, 5.0, 50.0 μM) and taking the equivalent volume of DMSO as the control at 100%. Compound **A1** and **F9** showed good inhibition on MPO-dependent LDL oxidation (62 ± 6, 4.5 ± 0.9, 11 ± 2% and 11 ± 2, 2.6 ± 0.8, 6 ± 4%, respectively), while no significant effect was detected for the other compounds.

**Transient-State Kinetics.** We further studied transient-state kinetics in order to determine the mechanism of inhibition. Two redox intermediates are relevant in the enzymology of MPO, namely compound I and compound II. Ferric MPO is oxidized by hydrogen peroxide into compound I, which is directly reduced back to the native state by chloride thereby producing hypochlorous acid.<sup>62,63</sup> Those reactions constitute the halogenation cycle. Alternatively, compound I can also be reduced back by two one-electron reduction steps via compound II (Figure 5). A good MPO inhibitor should (i) either efficiently block the entry to the heme cavity or (ii) promote formation of compound II, which is not competent in chlorination activity.<sup>57</sup>

We have preformed the two redox intermediates compound I and compound II<sup>47,62</sup> and probed their reactivity with the eight selected compounds. Figure 5 clearly demonstrates that all compounds acted as one-electron donors for compound I ( $k_2$ ) and compound II ( $k_3$ ) in monophasic reactions. Generally, all putative inhibitors reacted fast with compound I, with  $k_2$  values

ranging from  $6.8 \times 10^5 \text{ M}^{-1} \text{ s}^{-1}$  and  $4.1 \times 10^7 \text{ M}^{-1} \text{ s}^{-1}$ , respectively, whereas compound II reduction was still monophasic but significantly slower. As a consequence, compound II accumulated. The high discrepancy in reactivity of the putative inhibitors with compound I and compound II is underlined by the  $k_2/k_3$  ratios given in Table 3.

## DISCUSSION AND CONCLUSION

Using virtual screening of large databases of compounds has become a reliable strategy to identify new lead candidates in the drug discovery process. It is a complementary method to experimental approaches. Virtual screening involves molecular docking of the 3D structure of each ligand into the binding site of the target protein thereby generating a predicted binding mode whose fitness is evaluated. The obtained score is used in ranking of the compounds.

It is the first time that this approach has been carried out on MPO with such a large-scale database and without applying preselection criteria. A recent study described the virtual screening of 208 compounds extracted from the ZINC database<sup>58</sup> after filtering with a pharmacophore model based on the crystal structure of human MPO in complex with SHA.<sup>6</sup> As a consequence, structures forming interactions similar to SHA were found, i.e., stacking with the pyrrole ring D and hydrogen bonds with Gln91, His95, and Arg239.<sup>64</sup> Compared

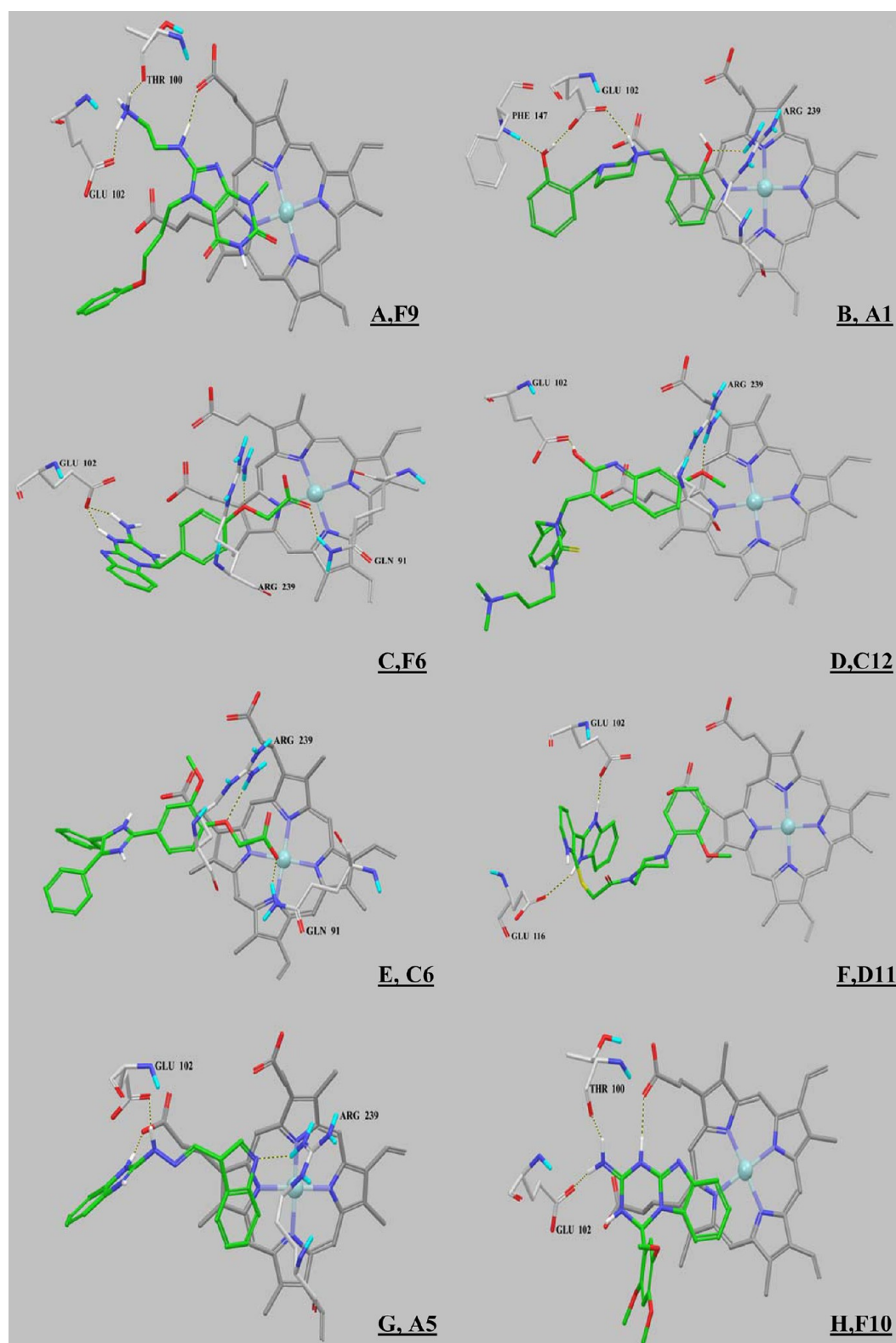


**Figure 4.** View of the docked positions of the eight compounds featuring the lowest  $IC_{50}$  on MPO. Hydrogen bonds and salt bridges are depicted as yellow–black dotted lines. (A) Compound F9, (B) compound A1, (C) compound F6, (D) compound C12, (E) compound C6, (F) compound D11, (G) compound A5, (H) compound F10.

to this study, the present work describes new scaffolds and new types of interactions with MPO.

Our calculations consisted of successive steps of docking including different levels of ligand selection (Figure 2). Starting from around 700000 molecules and 1350000 conformers, the

whole docking procedure selected 100 molecules, 81 of which were tested in vitro. Eight hits were then characterized in terms of inhibiting the oxidative modification of LDL by MPO. Moreover, their interaction with the redox intermediates compounds I and II were tested.

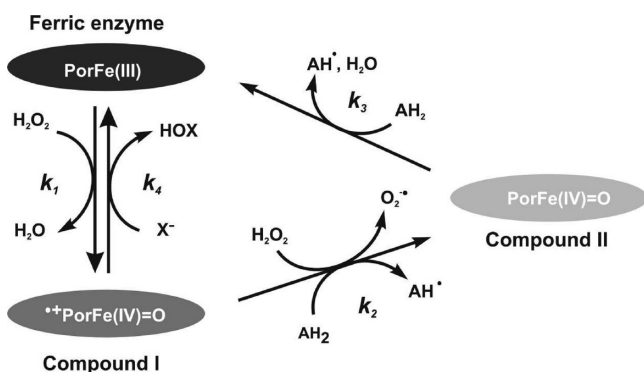


**Figure 5.** Schematic representation of the chlorination and peroxidase cycles of MPO. Reaction 1: ferric MPO is oxidized by hydrogen peroxide to compound I (i.e., oxoiron(IV) porphyrin radical cation). Reaction 2: compound I is reduced to compound II (i.e., protonated oxoiron(IV)) by a one-electron donor. Reaction 3: compound II is reduced to native state, thereby oxidizing a second substrate molecule. Reactions 1, 2, and 3 constitute the peroxidase cycle. Reaction 4: compound I is directly reduced back to the resting state by halides, thereby releasing hypohalous acid. Reactions (1) and (4) constitute the halogenation cycle.

**Table 3.** Apparent Bimolecular Rate Constants of MPO Compound I ( $k_2$ ) and Compound II Reduction ( $k_3$ ) by the Eight Selected Compounds<sup>a</sup>

compd	$k_2$ ( $M^{-1} s^{-1}$ )	$k_3$ ( $M^{-1} s^{-1}$ )	$k_2/k_3$
A5	$4.1 \times 10^7$	750 (E)	54667
F9	$5.1 \times 10^6$	210	24286
A1	$5.1 \times 10^6$	150 (E)	34000
C6	$1.9 \times 10^6$	10 (E)	190000
F10	$1.4 \times 10^6$	1.1	1272727
C12	$9.36 \times 10^5$	28 (E)	33429
F6	$6.8 \times 10^5$	27 (E)	25185
D11	ND	ND	ND

<sup>a</sup>Additionally, the  $k_2/k_3$  ratio is given. ND = no available data. (E) = estimated.

As for their predicted binding mode with MPO, the eight selected compounds feature one salt bridge with Glu102 and a stacking (shifted in a few cases) with pyrrole D of the prosthetic group. This emphasizes the importance of a positive charge and an aromatic moiety in potent MPO inhibitors. The importance of Glu102 has already been postulated for efficient binding of fluorotryptamine derivatives.<sup>49</sup> Compound A1 represents a new scaffold and could serve as a lead structure for MPO inhibition comprising interactions such as three hydrogen bonds with Glu102, Arg239, Phe147, and one salt bridge with Glu102. Compound F9 is one of the most potent inhibitor, and its purinedione structure has similarities with the structure of thioxanthine derivatives, which were patented as MPO inhibitors (Figure 6).<sup>50,51</sup> Among the other hit compounds, compound A5 which contains one indole ring is analogous to the already explored tryptamine derivatives.<sup>48,49</sup> Finally, compound C12 features a quinoline structure as the antimalarial drugs used as MPO inhibitors.<sup>37</sup>

Both new lead compounds act as electron donors of both compound I and compound II of MPO, but due to the differences in the oxidation capacity of the redox intermediates of MPO,<sup>13</sup> reaction with compound I was significantly faster ( $k_2 \gg k_3$ ). This suggests that the standard reduction potential of the selected MPO inhibitors is higher than 0.9 V.<sup>13</sup> As a

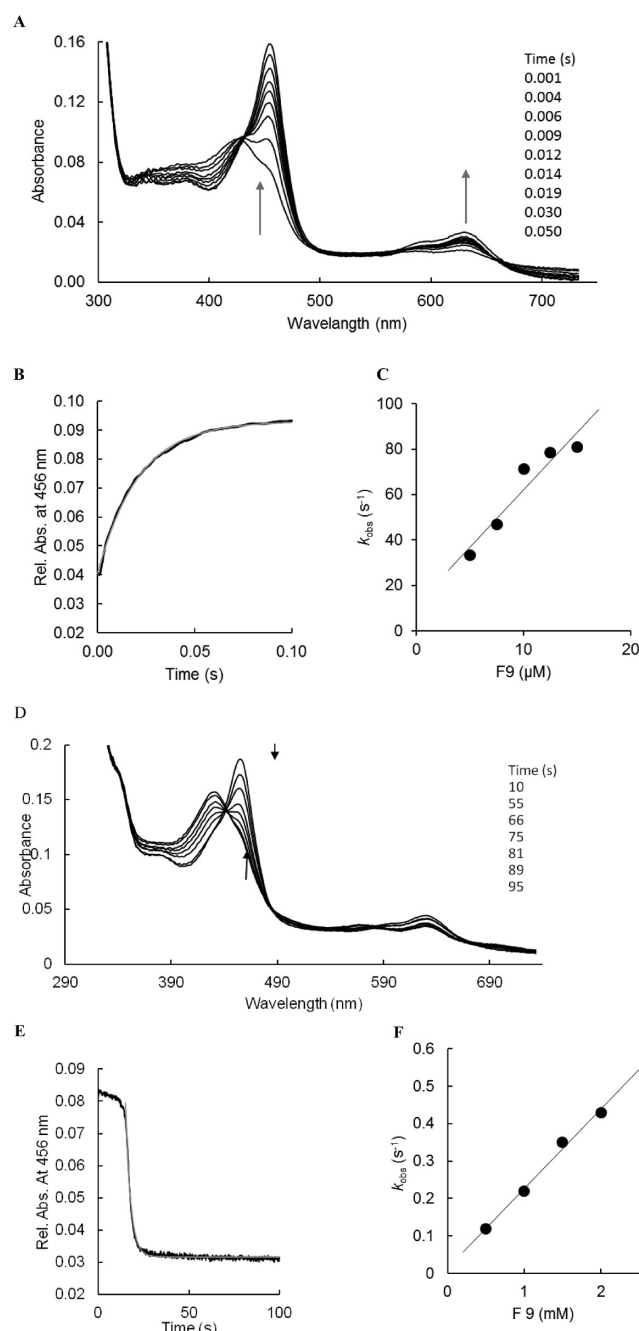


**Figure 6.** Reaction of MPO compound I with compound F9 (pH 7.4 and 25 °C). (A) Spectral changes upon reaction of 2  $\mu$ M MPO compound I with 10  $\mu$ M compound F9. (B) Typical time trace and fit of MPO compound II formation followed at 456 nm. (C) Pseudo-first-order rate constants for MPO compound I reduction plotted against F9 concentration. (D) Spectral changes upon reaction of 2  $\mu$ M MPO compound I with 500  $\mu$ M compound F9. (E) Typical time trace and fit of MPO compound II reduction with 2 mM F9 followed at 456 nm. (F) Pseudo-first-order rate constants for MPO compound II reduction plotted against F9 concentration.

consequence, the enzyme is trapped in the compound II state, which is outside the chlorination and bromination activity of this peroxidase. This mode of reversible inactivation of the chlorination and bromination activity has been shown with several other potent inhibitors.<sup>37,40–43,46–49,57</sup>

Functional scoring of ligand–protein complexes is mainly used to compare the relative affinity of different ligands or to

discriminate the “native-like” conformations of a ligand from the “non-native-like” ones. This scoring step remains very challenging and produces a correlation with experimental affinities which is not always optimal. As shown in Table 1, not all known potent MPO inhibitors would have been selected by our docking protocol. In the same way, among 81 compounds tested in the present work, 49 were totally inactive (60.5%), 32 were active (39.5%), and 8 compounds (i.e., 10%) inhibited more than 50% of the chlorination activity of MPO at 5  $\mu\text{M}$ .

One bottleneck in revealing the most essential receptor–ligand interactions for the inhibition mechanism is the lack of sufficient crystallographic data of complexes between MPO and promising lead compounds. So far, the MPO-SHA complex structure formed the basis for most of the studies.<sup>64</sup> Structural data of complexes with new scaffolds could clearly improve the selection of novel compounds because alternative selection criteria in HTVS could be applied.

In summing up, in this work eight active and reversible MPO inhibitors were selected. They act as electron donors of the oxidoreductase and efficiently block the halogenation activity without irreversible inactivation. Two of the selected compounds have a submicromolar activity and inhibit MPO-dependent LDL oxidation. In further steps, a pharmacomodulation on those hits should be endorsed to increase the inhibiting activity. The high-throughput virtual screening has thus been shown to be a successful tool to find new leads of MPO inhibitors. It improves the probability for finding new promising candidates at diminished time and expenses. Starting from a large-scale database, the process has allowed selecting original scaffolds of MPO inhibitors never explored so far.

## ■ EXPERIMENTAL SECTION: MATERIALS AND METHODS

**Docking Experiments. Preparation and Design of the MPO Receptor.** The X-ray structure of human MPO complexed to cyanide and thiocyanate (PDB code: 1DNW) was used as the target structure to endeavor the docking studies.<sup>7</sup> The PDB was prepared using the Protein Preparation Wizard protocol in the Schrodinger software graphical user interface Maestro including the usage of Epik 2.1109, Protassign 2.0.0, and Impact 56107. The X-ray water molecules in the catalytic site of MPO have been removed, and the charge of iron was set to +3. The structure was refined and optimized according to the following steps: (i) Only one monomer (chains A and C) was kept along with the heme and the cyanide anion close to the heme, (ii) all other molecules were removed (acetic acid,  $\alpha$ -D-mannose,  $\alpha$ -L-fucose, N-acetyl-D-glucosamine, thiocyanate ion, sulfate ion), (iii) the S-hydroxycysteine (150) was modified so as to generate a cysteine (Cys150), (iv) in agreement with the crystal structure, Asp94 and Glu242 were covalently bonded to the modified methyl groups of rings A and C of the heme through ester bonds, Met243 was also covalently bonded to the vinyl group of the heme (ring C) creating a sulfonium cation,<sup>63</sup> (v) following a  $pK_a$  calculation, Asp98 was protonated,<sup>63</sup> (vi) His95 was protonated on the N<sup>6</sup> to promote a hydrogen bond to the conserved Asp237 and to favor a proton transfer from hydrogen peroxide.<sup>63</sup> All hydrogens were added, and the whole structure was energy minimized. This final structure was used for the receptor grid generation (see next section).

**Receptor Grid Generation.** The final preparation step consisted of the definition of a cubic volume in which the shape and properties of the receptor (in absence of the cyanide) are represented on a grid by several different sets of force fields that provide progressively more sophisticated scoring of the ligand pose. This box, consisting of two embedded cubes (outer box and inner box), was centered on the position of the cyanide residue with a dimension of 26 Å for the larger box to contain the catalytic site of MPO. No constraints were placed

on the grids. The rotatable groups were assigned for the hydroxyl groups of Asp98, Thr100, and Thr238 (Figure 1).

**Preparing Ligands for the HTVS.** We chose to screen the ASINEX pharmaceutical database contained in the public Zinc database (Gold, Platinum, Synergy libraries).<sup>58</sup> The database consisted of 36 SDF files containing around 700000 molecules. Ligprep module from Schrodinger was used to prepare the ligands by generating the proper structures for docking, which included different tautomers and ionized forms prevalent at a pH range of  $7.0 \pm 2.0$ . The total number of ligands resulting from this procedure was 1350000 (Figure 2).

**Docking Procedure.** The Glide (Grid-Based Ligand Docking with Energetics) algorithm approximates a systematic search of positions, orientations, and conformations of the ligand in the receptor binding site using a series of hierarchical filters (www.schrodinger.com). The default settings of Glide version 5.6 were used. Three different Glide docking protocols and scoring function (HTVS, SP, and XP) were used to score the poses of the different ligands.

**In Vitro Inhibition Assays.** Recombinant MPO was prepared as previously described by Moguilevsky et al (1991).<sup>65</sup> Each batch solution is characterized by its protein concentration (mg/mL), its activity (U/mL), and its specific activity (U/mg). The chlorination activity was determined according to Hewson and Hager.<sup>66</sup>

**Myeloperoxidase Inhibition Assay.** The assay was based on the production of taurine chloramine produced by the MPO/H<sub>2</sub>O<sub>2</sub>/Cl<sup>-</sup> system in the presence of a selected inhibitor at defined concentration.<sup>60</sup> The reaction mixture contained the following reagents in a final volume of 200  $\mu\text{L}$ : 10 mM phosphate buffer, pH 7.4, 300 mM NaCl, 15 mM taurine, the compound to be tested (up to 20  $\mu\text{M}$ ), and the fixed amount of recombinant MPO (6.6  $\mu\text{L}$  of MPO batch solution diluted 2.5 times, 40 nM). When necessary, the volume was adjusted with water. This mixture was incubated at 37 °C and the reaction initiated with 10.0  $\mu\text{L}$  of H<sub>2</sub>O<sub>2</sub> from a 100  $\mu\text{M}$  stock solution. After 5 min, the reaction was stopped by addition of 10.0  $\mu\text{L}$  of catalase (8 U/ $\mu\text{L}$ ). To determine the amount of taurine chloramines produced, 50  $\mu\text{L}$  of 1.35 mM solution of thionitrobenzoic acid were added and the volume adjusted to 300  $\mu\text{L}$  with water. Then, the absorbance of the solutions was measured at 412 nm with a microplate reader and the curve of the absorbance as a function of the inhibitor concentration was plotted. IC<sub>50</sub> values were then determined using eight different concentrations between 0.1 and 16  $\mu\text{M}$ , taking the absence of hydrogen peroxide as 100% of inhibition and the absence of inhibitors as 0% of inhibition.<sup>41</sup> The calculation of the IC<sub>50</sub> has been done by linearization of the slope according to the equation ASIN ( $Y$ ) =  $a + b \times \text{LOG}_{10}(X)$  in Microsoft Office 2010. The values are the mean  $\pm$  SD of three independent measurements.

**Determination of LDL Oxidation Inhibition.** Human plasma served for the isolation of LDL by ultracentrifugation according to Havel et al.<sup>67</sup> Before oxidation, the LDL fraction ( $1.019 < d < 1.067$  g/mL) was desalted by two consecutive passages through PD10 gel-filtration columns (Amersham Biosciences, The Netherlands) using PBS buffer. The different steps were carried out in the dark, and the protein concentration was measured by the Lowry assay for both MPO and LDL.

LDL oxidation was carried out at 37 °C in a final volume of 500  $\mu\text{L}$ . The reaction mixture contained the following reagents at the final concentrations indicated between brackets: PBS buffer, pH 7.2, MPO (1  $\mu\text{g}/\text{mL}$ ), LDL (1000  $\mu\text{g}/\text{mL}$ ), 2  $\mu\text{L}$  1 M HCl (4 mM), one of the drugs at different concentrations, and H<sub>2</sub>O<sub>2</sub> (100  $\mu\text{M}$ ). The reaction was stopped after 5 min by cooling the tubes on ice. The assay was performed as described by Moguilevsky et al.<sup>68</sup> in a NUNC maxisorp plate (VWR, Zaventem, Belgium): 200 ng/well of LDL was coated overnight at 4 °C in a sodium bicarbonate pH 9.8 buffer (100  $\mu\text{L}$ )<sup>63</sup>

Afterward, the plate was washed with TBS 80 buffer and then saturated during 1 h at 37 °C with the PBS buffer containing 1% BSA (150  $\mu\text{L}/\text{well}$ ). After washing the wells twice with the TBS 80 buffer, the monoclonal antibody Mab AG9 (200 ng/well), obtained according to a standard protocol, was added as a diluted solution in PBS buffer with 0.5% BSA and 0.1% of Polysorbate 20.<sup>68</sup> After incubation for 1 h at 37 °C, the plate was washed four times with the TBS 80 buffer and a solution of IgG antimouse alkaline phosphatase (Promega, Leiden,



The Netherlands) diluted 3000 times in the same buffer was added (100  $\mu\text{L}/\text{well}$ ). The wells were washed again four times, and a revelation solution (150  $\mu\text{L}/\text{well}$ ) containing 5 mg of *para*-nitrophenyl phosphate in 5 mL of diethanolamine buffer was added for 30 min at room temperature. The reaction was stopped with 60  $\mu\text{L}/\text{well}$  of 3 N NaOH solution. The measurement of the absorbance was performed at 405 nm with a background correction at 655 nm with a Bio-Rad photometer for a 96-well plate (Bio-Rad laboratories, CA, USA).<sup>68</sup> Measurements were obtained by retrieving the effect of DMSO used for dissolving the compounds. Results were expressed as inhibition percentages.

**Transient State Kinetics.** Highly purified MPO of a purity index ( $A_{430}/A_{280}$ ) of a least 0.86 was purchased from Planta Natural Products (<http://www.planta.at>). Its concentration was calculated using  $\lambda_{430\text{ nm}} = 91\text{ mM}^{-1}\text{cm}^{-1}$ . Hydrogen peroxide, obtained from a 30% solution, was diluted and the concentration determined by absorbance measurement at 240 nm, where the extinction coefficient is 39.4  $\text{M}^{-1}\text{cm}^{-1}$ . Tested compounds stock solutions were prepared in dimethylsulfoxide (DMSO) and stored in dark flasks. Dilution was performed with 200 mM phosphate buffer, pH 7.4, to a final DMF concentration of 2% (v/v) in all assays.

The multimixing stopped-flow measurements were performed with the Applied Photophysics (UK) instrument SX-18MV. When 100  $\mu\text{L}$  were shot into a flow cell having a 1 cm light path, the fastest time for mixing two solutions and recording the first data point was 1.3 ms. Kinetics were monitored both at a single wavelength and by using a diode array detector. At least three determinations (2000 data points) of pseudo-first-order rate constants ( $k_{\text{obs}}$ ) were performed for each substrate concentration (pH 7.4, 25 °C), and the mean value was used in the calculation of the second-order rate constants, which were calculated from the slope of the line defined by a plot of  $k_{\text{obs}}$  versus substrate concentration. To allow calculation of pseudo-first-order rates, the concentrations of substrates were at least 10 times in excess of the enzyme.

Conditions of MPO compound I formation were described recently.<sup>63</sup> Typically, 8  $\mu\text{M}$  MPO were premixed with 80  $\mu\text{M}$   $\text{H}_2\text{O}_2$ , and after a delay time of 20 ms, compound I was allowed to react with varying concentrations of tested compounds in 200 mM phosphate buffer, pH 7.4. The reactions were followed at the Soret maximum of compound II (456 nm). Compound II formation and reduction could be followed in one measurement. The resulting biphasic curves at 456 nm showed the initial formation of compound II and its subsequent reduction to native MPO by the tested compounds (decrease in absorbance at 456 nm).

The samples which were analyzed for transient-state kinetics and compound I and compound II formation were dissolved in DMSO. When DMSO was interfering in the  $k_3$  calculation, we used instead the estimated value of  $k_3$ , which was calculated and estimated by using the spectrum of less concentrated solutions.

## ■ ASSOCIATED CONTENT

### ● Supporting Information

Close view of the docked positions of the eight compounds with a superimposition of 5-fluorotryptamine in the MPO active site,  $\text{IC}_{50}$  plots of the MPO inhibition assay, detailed information on the eight active compounds such as chemical structure, chemical name, physicochemical properties, and identification by high resolution mass spectrometry. This material is available free of charge via the Internet at <http://pubs.acs.org>.

## ■ AUTHOR INFORMATION

### Corresponding Author

\*Phone: +3226505263. Fax: +3226505249. E-mail: [pvantwer@ulb.ac.be](mailto:pvantwer@ulb.ac.be).

### Author Contributions

#Equally contributed to the manuscript

## Notes

The authors declare no competing financial interest.

## ■ ACKNOWLEDGMENTS

We thank the “Wallonie Bruxelles International” Agency ([www.wbi.be](http://www.wbi.be)) (grant no.: SOR/2011/33449) and the FRS-FNRS for their support (grant no. 34553.08). M.P. is a “Maître de Recherche” at the FNRS (Belgian Scientific Research Fund). Additionally, the work was supported by the Austrian Science Foundation (FWF project P1486).

## ■ ABBREVIATIONS USED

APO B-100, apolipoprotein B-100; DMSO, dimethylsulfoxide; HDL, high-density lipoprotein; HTVS, high-throughput virtual screening; LDL, low-density lipoprotein; NO, nitric oxide; Mox-LDL, low-density lipoproteins oxidized by myeloperoxidase; MPO, myeloperoxidase; SD, standard deviation; SHA, salicylhydroxamic acid; S, stacking; SP, Standard Precision; SS, shift stacking; XP, eXtra Precision

## ■ REFERENCES

- (1) Schultz, J.; Kaminker, K. Myeloperoxidase of the leucocyte of normal human blood. I. Content and localization. *Arch. Biochem. Biophys.* **1962**, *96*, 465–467.
- (2) Salmon, S. E.; Cline, M. J.; Schultz, J.; Lehrer, R. I. Myeloperoxidase Deficiency—Immunologic Study of a Genetic Leukocyte Defect. *N. Engl. J. Med.* **1970**, *282*, 250–253.
- (3) Zamocky, M.; Jakopitsch, C.; Furtmüller, P. G.; Dunand, C.; Obinger, C. The peroxidase–cyclooxygenase superfamily. Reconstructed evolution of critical enzymes of the innate immune system. *Proteins* **2008**, *71*, 589–605.
- (4) Zeng, J.; Fenna, R. E. X-ray crystal structure of canine myeloperoxidase at 3 Å resolution. *J. Mol. Biol.* **1992**, *226*, 185–207.
- (5) Andrews, P. C.; Krinsky, N. I. A kinetic analysis of the interaction of human myeloperoxidase with hydrogen peroxide, chloride ions, and protons. *J. Biol. Chem.* **1981**, *256*, 411–418.
- (6) Fiedler, T. J.; Davey, C. A.; Fenna, R. E. X-ray crystal structure and characterization of halide-binding sites of human myeloperoxidase at 1.8 Å. *J. Biol. Chem.* **2000**, *275*, 11964–11971.
- (7) Blair-Johnson, M.; Fiedler, T.; Fenna, R. Human myeloperoxidase: structure of a cyanide complex and its interaction with bromide and thiocyanate substrates at 1.9 Å resolution. *Biochemistry* **2001**, *40*, 13990–13997.
- (8) Van Antwerpen, P.; Slomianny, M. C.; Zouaoui Boudjeltia, K.; Delporte, C.; Faïd, V.; Calay, D.; Rousseau, A.; Moguilevsky, N.; Raes, M.; Vanhamme, L.; Furtmüller, P. G.; Obinger, C.; Vanheeverbeek, M.; Neve, J.; Michalski, J. C. Glycosylation pattern of mature dimeric leukocyte and recombinant monomeric myeloperoxidase: Glycosylation is required for optimal enzymatic activity. *J. Biol. Chem.* **2010**, *285*, 16351–16359.
- (9) Banerjee, S.; Stamper, J.; Furtmüller, P. G.; Obinger, C. Conformational and thermal stability of mature dimeric human myeloperoxidase and a monomeric recombinant form from CHO cells. *Biochim. Biophys. Acta* **2011**, *1814*, 375–387.
- (10) Klebanoff, S. J. Myeloperoxidase: Friend and foe. *J. Leukocyte Biol.* **2005**, *77*, 598–562.
- (11) Koeffler, H. P.; Ranyard, J.; Pertcheck, M. Myeloperoxidase: its structure and expression during myeloid differentiation. *Blood* **1985**, *65*, 484–491.
- (12) Yamada, M.; Kurahashi, K. Regulation of myeloperoxidase gene expression during differentiation of human myeloid leukemia HL-60 cells. *J. Biol. Chem.* **1984**, *259*, 3021–3025.
- (13) Arnhold, J.; Monzani, E.; Furtmüller, P. G.; Zederbauer, M.; Casella, L.; Obinger, C. Kinetics and thermodynamics of halide and nitrite oxidation by heme peroxidases. *Eur. J. Inorg. Chem.* **2006**, *19*, 3801–3811.

- (14) Zhang, R.; Brennan, M. L.; Shen, Z.; MacPherson, J. C.; Schmitt, D.; Molenda, C. E.; Hazen, S. L. Myeloperoxidase functions as a major enzymatic catalyst for initiation of lipid peroxidation at sites of inflammation. *J. Biol. Chem.* **2002**, *277*, 46116–46122.
- (15) Lane, A. E.; Tan, J. T.; Hawkins, C. L.; Heather, A. K.; Davies, M. J. The myeloperoxidase-derived oxidant HOSCN inhibits protein tyrosine phosphatases and modulates cell signalling via the mitogen-activated protein kinase (MAPK) pathway in macrophages. *Biochem. J.* **2010**, *15*, 161–169.
- (16) Choi, D. K.; Pennathur, S.; Perier, C.; Tieu, K.; Teismann, P.; Wu, D. C.; Jackson-Lewis, V.; Vila, M.; Vonsattel, J. P.; Heinecke, J. W.; Przedborski, S. Ablation of the inflammatory enzyme myeloperoxidase mitigates features of Parkinson's disease in mice. *J. Neurosci.* **2005**, *25*, 6594–6600.
- (17) Maki, R. A.; Tyurin, V. A.; Lyon, R. C.; Hamilton, R. L.; Dekosky, S. T.; Kagan, V. E.; Reynolds, W. F. Aberrant expression of myeloperoxidase in astrocytes promotes phospholipid oxidation and memory deficits in a mouse model of Alzheimer's disease. *J. Biol. Chem.* **2009**, *284*, 3158–3169.
- (18) Matthijssen, R. A.; Huugen, D.; Hoebbers, N. T.; de Vries, B.; Peutz-Kootstra, C. J.; Aratani, Y.; Daha, M. R.; Tervaert, J. W.; Buurman, W. A.; Heeringa, P. Myeloperoxidase is critically involved in the induction of organ damage after renal ischemia reperfusion. *Am. J. Pathol.* **2007**, *171*, 1743–1752.
- (19) Reynolds, W. F.; Hiltunen, M.; Pirskanen, M.; Mannermaa, A.; Helisalini, S.; Lehtovirta, M.; Alafuzoff, I.; Soininen, H. MPO and APOEepsilon4 polymorphisms interact to increase risk for AD in Finnish males. *Neurology* **2000**, *55*, 1284–90.
- (20) Reynolds, W. F.; Rhee, J.; Maciejewski, D.; Paladino, T.; Sieburg, H.; Maki, R. A.; Masliah, E. Myeloperoxidase polymorphism is associated with gender specific risk for Alzheimer's disease. *Exp. Neurol.* **1999**, *155*, 31–41.
- (21) Sawayama, Y.; Miyazaki, Y.; Ando, K.; Horio, K.; Tsutsumi, C.; Imanishi, D.; Tsushima, H.; Imaizumi, Y.; Hata, T.; Fukushima, T.; Yoshida, S.; Onimaru, Y.; Iwanaga, M.; Taguchi, J.; Kuriyama, K.; Tomonaga, M. Expression of myeloperoxidase enhances the chemosensitivity of leukemia cells through the generation of reactive oxygen species and the nitration of protein. *Leukemia* **2008**, *22*, 956–964.
- (22) El Kebir, D.; József, L.; Pan, W.; Filep, J. G. Myeloperoxidase delays neutrophil apoptosis through CD11b/CD18 integrins and prolongs inflammation. *Circ. Res.* **2008**, *103*, 352–359.
- (23) Hirche, T. O.; Gaut, J. P.; Heinecke, J. W.; Belaouaj, A. Myeloperoxidase plays critical roles in killing *Klebsiella pneumoniae* and inactivating neutrophil elastase: effects on host defense. *J. Immunol.* **2005**, *174*, 1557–1565.
- (24) Lau, D.; Mollnau, H.; Eiserich, J. P.; Freeman, B. A.; Daiber, A.; Gehling, U. M.; Brummer, J.; Rudolph, V.; Munzel, T.; Heitzer, T.; Meinertz, T.; Baldus, S. Myeloperoxidase mediates neutrophil activation by association with CD11b/CD18 integrins. *Proc. Natl. Acad. Sci. U.S.A.* **2005**, *102*, 431–436.
- (25) Green, P. S.; Mendez, A. J.; Jacob, J. S.; Crowley, J. R.; Growdon, W.; Hyman, B. T.; Heinecke, J. W. Neuronal expression of myeloperoxidase is increased in Alzheimer's disease. *J. Neurochem.* **2004**, *90*, 724–33.
- (26) Nagra, R. M.; Becher, B.; Tourtellotte, W. W.; Antel, J. P.; Gold, D.; Paladino, T.; Smith, R. A.; Nelson, J. R.; Reynolds, W. F. Immunohistochemical and genetic evidence of myeloperoxidase involvement in multiple sclerosis. *J. Neuroimmunol.* **1997**, *78*, 97–107.
- (27) Nicholls, S. J.; Hazen, S. L. Myeloperoxidase and cardiovascular disease. *Arterioscler. Thromb. Vasc. Biol.* **2005**, *25*, 1102–1111.
- (28) Roman, R. M.; Wendland, A. E.; Polanczyk, C. A. Myeloperoxidase and coronary arterial disease: from research to clinical practice. *Arq. Bras. Cardiol.* **2008**, *91*, e11–9.
- (29) Daugherty, A.; Rateri, D. L.; Dunn, J. L.; Heinecke, J. W. Myeloperoxidase, a catalyst for lipoprotein oxidation, is expressed in human atherosclerotic lesions. *J. Clin. Invest.* **1994**, *94*, 437–444.
- (30) Malle, E.; Marsche, G.; Panzenboeck, U.; Sattler, W. Myeloperoxidase-mediated oxidation of high-density lipoproteins: fingerprints of newly recognized potential proatherogenic lipoproteins. *Arch. Biochem. Biophys.* **2006**, *445*, 245–255.
- (31) Itabe, H. Oxidative modification of LDL: its pathological role in atherosclerosis. *Clin. Rev. Allergy Immunol.* **2009**, *37*, 4–11.
- (32) Zouaoui-Boudjeltia, K.; Legssyer, I.; Van Antwerpen, P.; Lema Kisoka, R.; Babar, S.; Moguilevsky, N.; Delree, P.; Ducobu, J.; Remacle, C.; Vanhaeverbeek, M.; Brohee, D. Triggering of inflammatory response by myeloperoxidase-oxidized LDL. *Biochem. Cell Biol.* **2006**, *84*, 805–812.
- (33) Exner, M.; Minar, E.; Mlekusch, W.; Sabeti, S.; Amighi, J.; Lalouschek, W.; Maurer, G.; Bieglmayer, C.; Kieweg, H.; Wagner, O.; Schillinger, M. Myeloperoxidase predicts progression of carotid stenosis in states of low high-density lipoprotein cholesterol. *J. Am. Coll. Cardiol.* **2006**, *47*, 2212–2218.
- (34) Steinberg, D.; Parthasarathy, S.; Carew, T. E.; Khoo, J. C.; Witztum, J. L. Beyond cholesterol. Modifications of low-density lipoprotein that increase its atherogenicity. *New Engl. J. Med.* **1989**, *320*, 915–924.
- (35) O'Brien, K. D.; Alpers, C. E.; Hokanson, J. E.; Wang, S.; Chait, A. Oxidation specific epitopes in human coronary atherosclerosis are not limited to oxidized low-density lipoprotein. *Circulation* **1996**, *94*, 1216–1225.
- (36) Marsche, G.; Hammer, A.; Oskolkova, O.; Kozarsky, K. F.; Sattler, W.; Malle, E. Hypochlorite-modified high density lipoprotein, a high affinity ligand to scavenger receptor class B, type I, impairs high density lipoprotein dependent selective lipid uptake and reverse cholesterol transport. *J. Biol. Chem.* **2002**, *277*, 32172–32179.
- (37) Kettle, A. J.; Winterbourn, C. C. Mechanism of inhibition of myeloperoxidase by anti-inflammatory drugs. *Biochem. Pharmacol.* **1991**, *41*, 1485–1492.
- (38) Van Zyl, A.; Lubbe, S.; Potgieter, A.; Van Zyl, J. The influence of non-steroidal anti-inflammatory and antithyroid agents on myeloperoxidase-catalysed activities of human leucocytes. *S. Afr. Med. J.* **1979**, *55*, 1082–1087.
- (39) Van Antwerpen, P.; Dufrasne, F.; Lequeux, M.; et al. Inhibition of the myeloperoxidase chlorinating activity by non-steroidal anti-inflammatory drugs: flufenamic acid and its 5-chloro-derivative directly interact with a recombinant human myeloperoxidase to inhibit the synthesis of hypochlorous acid. *Eur. J. Pharmacol.* **2007**, *570*, 235–243.
- (40) Nève, J.; Parij, N.; Moguilevsky, N. Inhibition of the myeloperoxidase chlorinating activity by non-steroidal anti-inflammatory drugs investigated with a human recombinant enzyme. *Eur. J. Pharmacol.* **2001**, *417*, 37–43.
- (41) Van Antwerpen, P.; Prévost, M.; Zouaoui-Boudjeltia, K.; Babar, S.; Legssyer, I.; Moreau, P.; Moguilevsky, N.; Vanhaeverbeek, M.; Ducobu, J.; Nève, J.; Dufrasne, F. Conception of myeloperoxidase inhibitors derived from flufenamic acid by computational docking and structure modification. *Bioorg. Med. Chem.* **2008**, *16*, 1702–1720.
- (42) Shiba, Y.; Kinoshita, T.; Chuman, H.; Taketani, Y.; Takeda, E.; Kato, Y.; Naito, M.; Kawabata, K.; Ishisaka, A.; Terao, J.; Kawai, Y. Flavonoids as substrates and inhibitors of myeloperoxidase: molecular actions of aglycone and metabolites. *Chem. Res. Toxicol.* **2008**, *21*, 1600–1609.
- (43) Davies, B.; Edwards, S. W. Inhibition of myeloperoxidase by salicylhydroxamic acid. *Biochem. J.* **1989**, *258*, 801–806.
- (44) Kettle, J.; Gedye, C.; Hampton, M.; Winterbourn, C. Inhibition of myeloperoxidase by benzoic acid hydrazides. *Biochem. J.* **1995**, *308*, 559–563.
- (45) Burner, U.; Obinger, C.; Paumann, M.; Furtmüller, P. G.; Kettle, A. J. Transient-state and steady-state kinetics of the oxidation of benzoic acid hydrazides by myeloperoxidase. *J. Biol. Chem.* **1999**, *274*, 9494–9502.
- (46) Allegra, M.; Furtmüller, P. G.; Regelsberger, G.; Turco-Liveri, M. L.; Tesoriere, L.; Perretti, M.; Livrea, M. A.; Obinger, C. Mechanism of reaction of melatonin with human myeloperoxidase. *Biochem. Biophys. Res. Commun.* **2001**, *282*, 380–386.
- (47) Jantschko, W.; Furtmüller, W.; Allegra, M.; Livrea, M. A.; Jakopitsch, C.; Regelsberger, G.; Obinger, C. Redox intermediates of plant and mammalian peroxidases: a comparative transient-kinetic

study of their reactivity toward indole derivatives. *Arch. Biochem. Biophys.* **2002**, *398*, 12–22.

(48) Jantschko, W.; Furtmüller, P. G.; Zederbauer, M.; Neugschwandtner, K.; Lehner, I.; Jakopitsch, C.; Arnhold, J.; Obinger, C. Exploitation of the unusual thermodynamic properties of human myeloperoxidase in inhibitor design. *Biochem. Pharmacol.* **2005**, *69*, 1149–1157.

(49) Soubhye, J.; Prévost, M.; Van Antwerpen, P.; Zouaoui Boudjeltia, K.; Rousseau, A.; Furtmüller, P. G.; Obinger, C.; Vanhaeverbeek, M.; Ducobu, J.; Néve, J.; Gelbcke, M.; Dufasne, F. O. Structure-based design, synthesis, and pharmacological evaluation of 3-(aminoalkyl)-5-fluoroindoles as myeloperoxidase inhibitors. *J. Med. Chem.* **2010**, *53*, 8747–59.

(50) Tidén, A. K.; Sjögren, T.; Svensson, M.; Bernlind, A.; Senthilmohan, R.; Auchère, F.; Norman, H.; Markgren, P. O.; Gustavsson, S.; Schmidt, S.; Lundquist, S.; Forbes, L. V.; Magon, N. J.; Paton, L. N.; Jameson, G. N.; Eriksson, H.; Kettle, A. J. 2-Thioxanthines are mechanism-based inactivators of myeloperoxidase that block oxidative stress during inflammation. *J. Biol. Chem.* **2011**, *286*, 37578–37589.

(51) Hanson, S.; Nordvall, G.; Tiden, A. K. Preparation of xanthine derivatives as myeloperoxidase inhibitors. PCT Int. Appl. WO 2003089430 A1 20031030, 2003.

(52) Choi, D. K.; Koppula, S.; Choi, M.; Suk, K. Recent developments in the inhibitors of neuroinflammation and neurodegeneration: inflammatory oxidative enzymes as a drug target. *Expert Opin. Ther. Pat.* **2010**, *20*, 1531–46.

(53) Bogevig, A.; Lo-Alfredsson, Y.; Pivonka, D.; Tiden, A. K. Pyrrolo [3,2-*d*]pyrimidin-4-one derivatives and their use in therapy. U.S. Patent US007829707B2, 2010.

(54) Svensson, M.; Tiden, A. K.; Turek, D. Use of derivatives of 2,4-dihydro-[1,2,4]triazole-3-thione as inhibitors of the enzyme myeloperoxidase (MPO). U.S. Patent US 20070093483A1, 2007.

(55) Lojek, A.; Cíž, M.; Pekarová, M.; Ambrožová, G.; Vašíček, O.; Moravcová, J.; Kubala, L.; Drábiková, K.; Jančinová, V.; Perečko, T.; Pečivová, J.; Mačičková, T.; Nosál, R. Modulation of metabolic activity of phagocytes by antihistamines. *Interdiscip. Toxicol.* **2011**, *4*, 15–19.

(56) Egan, R. W.; Hagmann, W. K.; Gale, P. H. Agents Actions. Naphthalenes as inhibitors of myeloperoxidase: direct and indirect mechanisms of inhibition. *Agents Actions* **1990**, *29*, 266–276.

(57) Malle, E.; Sattler, W.; Furtmüller, P. G.; Obinger, C. Myeloperoxidase: a new target for drug development? *Br. J. Pharmacol.* **2007**, *152*, 838–854.

(58) Irwin, J. J.; Shoichet, B. K. ZINC—a free database of commercially available compounds for virtual screening. *J. Chem. Inf. Model.* **2005**, *45*, 177–182.

(59) Davey, C. A.; Fenna, R. E. 2.3 Å Resolution X-ray Crystal Structure of the Bisubstrate Analogue Inhibitor Salicylhydroxamic Acid Bound to Human Myeloperoxidase: A Model for a Prereaction Complex with Hydrogen Peroxide. *Biochemistry* **1996**, *35*, 10967–10973.

(60) Van Antwerpen, P.; Moreau, P.; Zouaoui-Boudjeltia, K.; Babar, S.; Dufasne, F.; Moguilevsky, N.; Vanhaeverbeek, M.; Ducobu, J.; Neve, J. Development and validation of screening procedure for the assessment of inhibition using a recombinant enzyme. *Talanta* **2007**, *75*, 503–510.

(61) Van Antwerpen, P.; Boudjeltia-Zouaoui, K.; Babar, S.; Legssyer, I.; Moreau, P.; Moguilevsky, N.; Vanhaeverbeek, M.; Ducobu, J.; Neve, J. Thiol-containing molecules interact with the myeloperoxidase/H<sub>2</sub>O<sub>2</sub>/chloride system to inhibit LDL oxidation. *Biochem. Biophys. Res. Commun.* **2005**, *337*, 82–88.

(62) Furtmüller, P. G.; Burner, U.; Obinger, C. Reaction of human myeloperoxidase compound I with chloride, bromide, iodide, and thiocyanate. *Biochemistry* **1998**, *37*, 17923–17930.

(63) Furtmüller, P. G.; Zederbauer, M.; Jantschko, W.; Helm, J.; Bogner, M.; Jakopitsch, C.; Obinger, C. Active site structure and catalytic mechanisms of human peroxidases. *Arch. Biochem. Biophys.* **2006**, *445*, 199–213.

(64) Malvezzi, A.; Queiroz, R. F.; De Rezende, L.; Augusto, O.; do Amaral, A. T. MPO Inhibitors Selected by Virtual Screening. *Mol. Inform.* **2011**, *30*, 605–613.

(65) Moguilevsky, N.; Garcia-Quintana, L.; Jacquet, A.; Tournay, C.; Fabry, L.; Piérard, L.; Bollen, A. Structural and biological properties of human recombinant myeloperoxidase produced by Chinese hamster ovary cell lines. *Eur J Biochem.* **1991**, *197*, 605–614.

(66) Hewson, W. D.; Hager, L. P. Mechanism of the chlorination reaction catalyzed by horseradish peroxidase with chlorite. *J. Biol. Chem.* **1979**, *254*, 3175–3181.

(67) Havel, R. J.; Eder, H. A.; Bragdon, J. H. Distribution and chemical composition of ultracentrifugally separated lipoproteins in human serum. *J. Clin. Invest.* **1955**, *34*, 1345–1353.

(68) Moguilevsky, N.; Zouaoui-Boudjeltia, Z.; Babar, S.; Delree, P.; Legssyer, I.; Carpentier, Y.; Vanhaeverbeek, M.; Ducobu, J. Monoclonal antibodies against LDL progressively oxidized by myeloperoxidase react with ApoB-100 protein moiety and human atherosclerotic lesions. *Biochem. Biophys. Res. Commun.* **2004**, *323*, 1223–1228.

#### ■ NOTE ADDED AFTER ASAP PUBLICATION

After this paper was published online August 7, 2012, changes were made to the references throughout. The revised version was reposted August 10, 2012.